Proceedings of the 9th U.S. National and 10th Canadian Conference on Earthquake Engineering
Compte Rendu de la 9ième Conférence Nationale Américaine et
10ième Conférence Canadienne de Génie Parasismique
July 25-29, 2010, Toronto, Ontario, Canada • Paper No 159

ANALYSIS AND TESTING OF CABLES MADE OF CUALBE SMA

J. F. Beltran[1], C. Cruz[2], M.O. Moroni[3] and R. Herrera[1]

ABSTRACT

Copper based shape memory alloys (SMA) possess thermo-mechanical properties that make them ideal for energy dissipation and re-centering devices for structural applications. However, good dissipation and re-centering characteristics have only been achieved for small diameter SMA wires and rods tested as single elements in tension or in small scale models tested in shaking tables. Attempts to achieve the same characteristics for sizes required in real structures have been unsuccessful.
The use of structural cables made of SMA wires is an alternative of application of this material to civil structures. Structural cables are composed of wires helically wound into strands, which, in turn, are wound around a core. They have high redundancy and can be used to carry large tensile forces in many civil engineering structures. If the cable is composed of SMA wires in austenite phase, better dissipation and/or re-centering capacity can be expected. Strand specimens were constructed from CuAlBe SMA wires and tested under cyclic tension. The specimens included helically wound strands and groups of wires in parallel. Strand experimental results are then used to validate a computational model developed to estimate cable response under axisymmetric loads.

Introduction

Copper based shape memory alloys (SMA) possess thermo-mechanical properties that make them ideal for energy dissipation and re-centering devices for structural applications. However, good dissipation and re-centering characteristics have only been achieved for small diameter SMA wires and rods tested as single elements in tension or in small scale models tested in shaking tables. Attempts to achieve the same characteristics for sizes required in real structures have been unsuccessful.

The use of structural cables made of SMA wires is an alternative of application of this material to civil structures. In general, a cable is constructed by twisting a group of strands elements or wires around a straight core (twisted wire cables). They have high redundancy and can be used to carry large tensile forces in many civil engineering structures. If the cable is composed of SMA wires in austenite phase, better dissipation and/or re-centering capacity can be expected.

Reedlunn and Shaw (2008) performed some experiments on two commercially available Nitinol cables. The specimens were uniaxially loaded and infrared imaging was used to monitor transformation activity. The elongation rate was rather low. The response qualitatively matches the typical behaviour of

[1]Assistant Professor, Dept. of Civil Engineering, University of Chile, Santiago, Chile
[2]Graduate Student, Dept. of Civil Engineering, University of Chile, Santiago, Chile.
[3]Associate Professor, Dept. of Civil Engineering, University of Chile, Santiago, Chile

NiTi wire when the helix angle is low, but it differs substantially for a larger helix angle. Also remnant deformation are larger.

In this research, mechanical experiments were performed on strands made of CuAlBe SMA wires to characterize their behaviour and demonstrate their potential utility as resilient tension elements. In particular, parallel and twisted strands were uniaxially loaded and from the stress-strain curves equivalent viscous damping (ξ) and forward transformation (σ_t) and ultimate stresses (σ_u) were determined for each maximum strain. Later, strand experimental results are used to validate a computational model developed to estimate cable response under axisymmetric loads. Equilibrium equations are established for each individual wire, wire geometry is linearized, and a multilinear SMA CuAlBe wire stress-strain curve is used for computational purposes. Relationships between individual wire and strand properties were derived, and comparisons were made between strands with parallel and helical configuration.

Wires Characteristics

Wires 0.5 mm diameter were previously tested under both quasi-static and dynamic tensile loading and reported elsewhere (Araya et al 2008). A summary is presented here.

The wires were heat-treated during different periods of time, and tested to study the effect of grain size, temperature, and strain rate on the strength, equivalent viscous damping, and re-centering properties of the alloy. The nominal composition was Cu-11.8wt.%Al-0.5wt.%Be, furnished by Trefimétaux, France. Phase transformation temperatures reported by the manufacturer are M_f = -47ºC, M_s = -18ºC, A_s = -20ºC and A_f = 2ºC. Since ambient temperatures for civil engineering structures are usually greater than the A_f transition temperature of 2 ºC, the material is expected to operate within its superelastic range.

The test samples were 90 mm long, while the distance between the machine grips was about 70 mm. The cyclic tests were performed for nominal strain amplitudes of 0.8, 1.5 and 2.2 % and for temperatures ranging from 6 °C to 50 °C. The strain was measured with an extensometer that has a 25 mm gauge length. The wires were initially slightly prestressed to avoid buckling. Each sample was tested at one amplitude with the following temperature sequence 25º, 6º, 50º, 25º, 6º and 50ºC. Later, some samples were retested at 25ºC up to fracture. Most of the tests consisted of series of 20 cycles at defined nominal strain amplitudes. To observe the evolution of the hysteresis cycles, some of the series included up to 60 cycles.

Fig. 1 shows cyclic tensile curves obtained for a nominal strain amplitude of 2.2% at 1 Hz, and for different grain sizes and temperatures. In each case, series of 20 cycles were imposed; for clarity sake only the stress-strain of the second cycle is given; actually, the first cycle was somewhat different from the others, while all the rest are very close to each other.

The following remarks can be drawn from cyclic tests:

- The material shows superelasticity. Actually, within experimental strains error limits, no residual deformations were detected under the employed tests conditions, although retained martensite was observed in optical microscopy images taken after the tests and not shown here.
- For a given grain size, s_t and the effective stiffness increase for increasing temperatures. The effective stiffness, a relevant civil-engineering design parameter, is defined for each cycle as the ratio $(\sigma_{max}-\sigma_{min})/(\varepsilon_{max}-\varepsilon_{min})$.
- Effective stiffness and forward transformation stress decrease for larger grain size.
- For a given grain size, the maximum stress increases and the maximum strain diminishes as temperature is increased. This behaviour is related to the effect of temperature on the flow stress curve and to the type of strain control used in the tests. As it was pointed out, for higher

temperature the material is stiffer, therefore, for the same load, less deformation is attained.

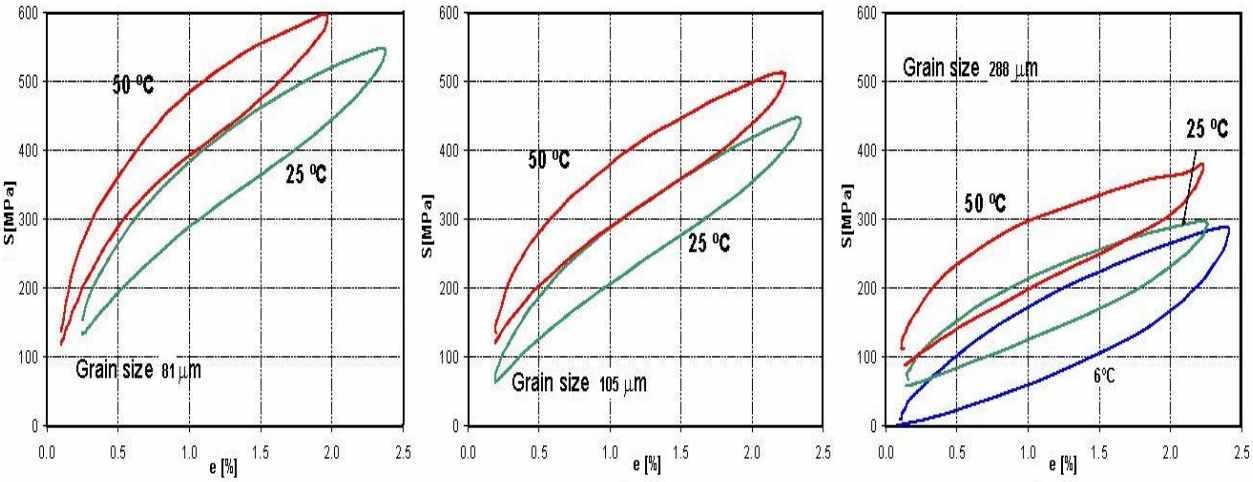

Figure 1. Stress-strain relationship, for different grain size and temperature

Fig. 2 shows the equivalent viscous damping, calculated as the energy loss per cycle divided by (4π maximum strain energy per cycle), as a function of the grain size for 2.2% nominal strain amplitude. For all grain sizes, a smaller equivalent damping is obtained for higher temperatures; moreover, damping is larger for larger grain sizes. However, larger grain sizes means less number of grains per diameter, so a less redundancy situation is generated.

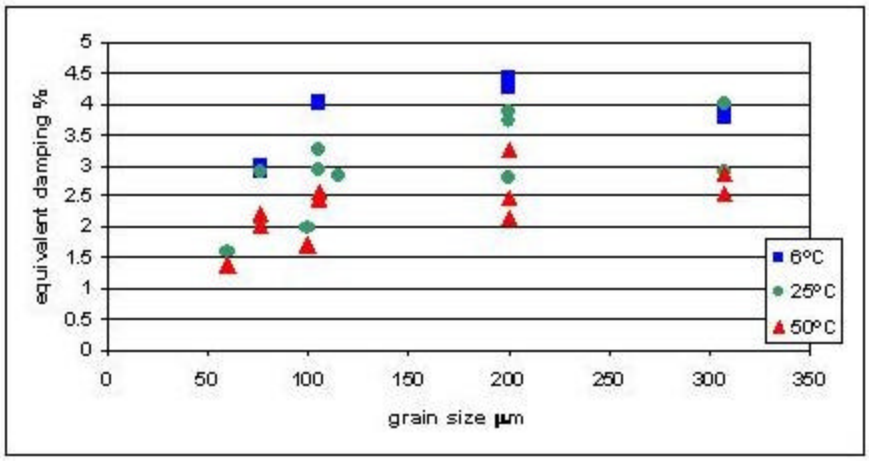

Figure 2. Equivalent damping 0.5 mm wires

Strand Experimental Tests

Two 1 x 19 x 0.5 mm strand specimens 15 cm long were constructed from the previous CuAlBe wires, heat treated at 700ºC during 20 sec resulting in a nominal grain size of 60 μm. The nominal outer diameter was 2.5 mm. The helix angle of the exterior wires was 17.5º. Other two specimens included 19 wires in parallel, 15 cm long. The four of them were tested under cyclic tension at the Structural Engineering and Material Research Laboratory, Georgia Tech. The specimens were uniaxially loaded by an MTS electromechanical load frame, using a 50 kN load cell to monitor the force, while the grip displacement was measured by internal LVDT.

Two patterns of controlled displacements were applied: 20 cycles up to 2% strain and 22 cycles with amplitudes varying from 0.5% till 8%. In the latter, the following sequence was followed: 3 cycles at 0.5%, 1 cycle at 0.8%, 1.0 %, and 1.5%, 5 cycles at 2.2%, 1 cycle at 2.5, 3.0, 3.5, 4.0 and 4.5%, 5 cycles at 5.0% and 1 cycle at 8.0%. The strain rate was 0.1 mm/sec. For all specimens, the initial distance between the grips was about 10 cm, at zero loads.

Figure 3 shows stress-strain relationship for the strand and the parallel wires subjected to 20 cycles at 2% strain, the curves are quite similar to those obtained for a single wire. Figure 4 shows the curves for increasing strains and the monotonic curve obtained for a single wire tested at 25ºC. The axial stress on each cable specimen is reported as P/A_o where ($A_o = n\pi d^2/4$) is a chosen reference area based on the number of wires (n) in the cable and the individual wire diameter (d) (Reedlunn and Shaw,2008).

From these curves, elasticity modulus, forward transformation stress and equivalent viscous damping were calculated. Table 1 shows the elasticity modulus and the forward transformation and ultimate stresses for the different strands and single wires. Figure 5 shows the variation of equivalent viscous damping with strain for both cables and individual wires. Again, equivalent viscous damping is rather low.

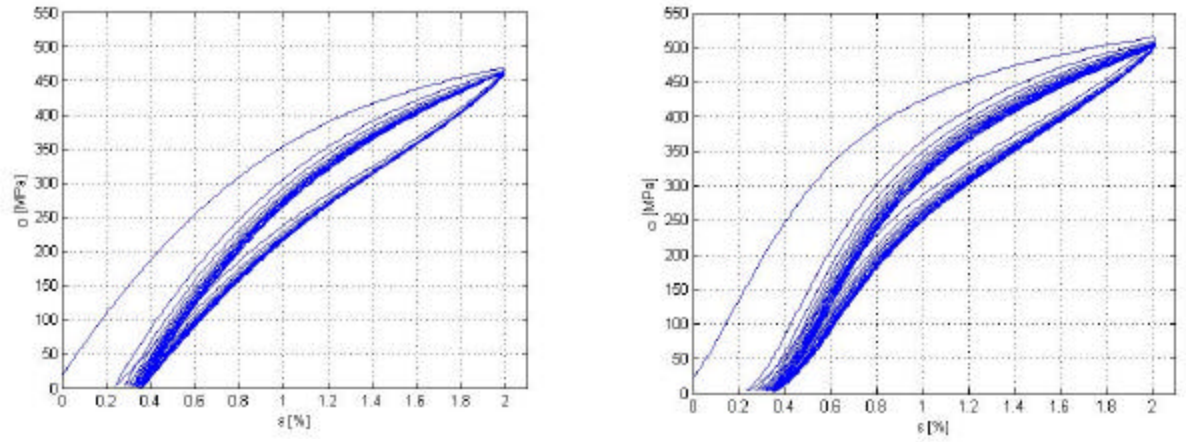

(a) helical strand (b) parallel wires

Figure 3. Stress-strain curves. 20 cycles at 2% strain

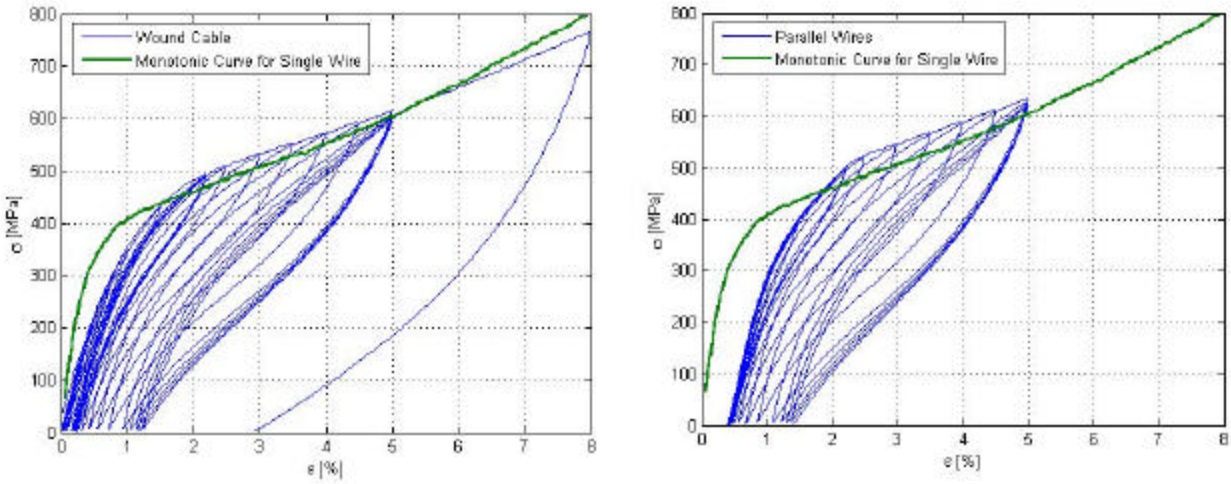

(a) helical strand (b) parallel wires

Figure 4. Stress-strain curves. 22 cycles at increasing strains

Table 1. Elasticity Modulus, forward transformation and ultimate stresses

Specimen	E	σ_t	σ_u
Strand 2%	48.8 GPa	225.5 MPa	460.9 MPa
Parallel 2%	56.3 GPa	301.5 MPa	501.2 MPa
Strand 5%	37.1 GPa	242.7 MPa	605.8 MPa
Parallel 5%	40.3 GPa	263.3 MPa	625.3 MPa
Wire 0.8%	99.0 GPa	300.0 MPa	441.0 MPa
Wire 1.5%	79.0 GPa	270.0 MPa	493.0 MPa
Wire 2.2 %	52.0 GPa	240.0 MPa	546.0 MPa

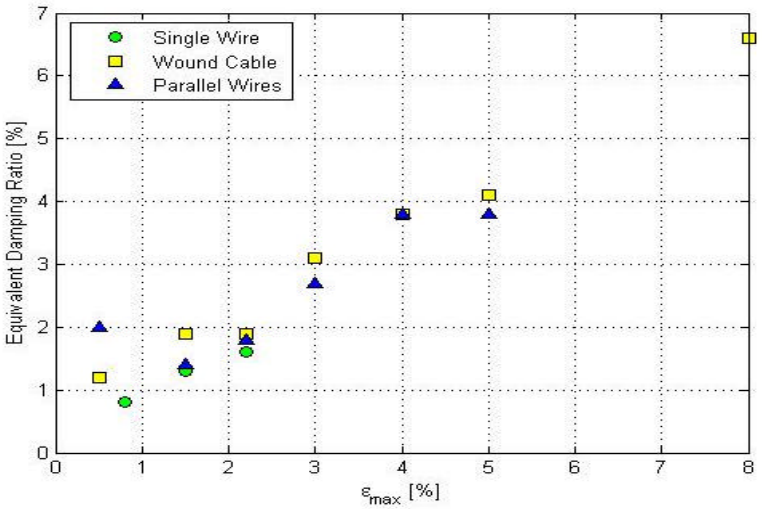

Figure 5. Equivalent viscous damping

Cable Analytical Model

In general, a cable is constructed by twisting a group of cable elements or wires around a straight core (twisted wire cables). A wire is a structural element whose cross-section is small compared to its length. The so-called plane-sections hypothesis is assumed: rope element cross-sections that are plane before deformation remain plane after deformation, thus the motion of a rope element is described in terms of parameters that are a function of only its axial coordinate. It is assumed that in the deformed and initial configurations, the geometry of a rope element, represented by its centerline (longitudinal or helix axis), can be described by a circular helix curve. Three geometric parameters are needed to describe a wire in a single helix configuration: helix radius (a), projected length of the rope component on the core axis (L) and pitch distance (p) as shown in Fig. 6. The helix radius is the distance measured from the core axis to the centerline of the wire and the pitch distance of a wire is the distance along the core component measured for a variation of a swept angle that varies from 0 to 2p. By definition, a circular helix curve makes a constant angle (helix angle) with a fixed line in space. This fixed line is the longitudinal axis of each component, and the helix angle (?) is defined as the angle between the axis of the component and the axis of the core component (Fig 6). The helix angle (?) can be computed using the following expression:

$$\tan(q) = \frac{2pa}{p} \tag{1}$$

Due to its helical nature, a twisted wire cable possesses nonlinear strain-displacement

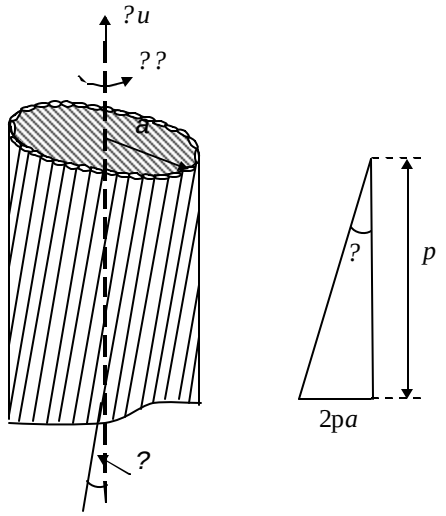

Fig. 6. Cable Geometry

relationships and its axial behavior exhibits coupling between tension and torsion. Velinsky (1985) presented a general discrete geometrical nonlinear theory to simulate twisted ropes behavior with complex cross-sections in their linear-elastic regime. The results of the proposed theory were compared to its linearized version and experimental data. The linear theory is based on the linearization of the strain-displacement relationships of a cable wire and the initial cable configuration is considered as the reference configuration. Linear models can essentially be divided into two categories, which are based on the types of hypotheses employed: (a) fiber models where the wire ropes can develop only tensile forces, and (b) rod models where the wire ropes can develop tensile and shear forces as well as

bending and twisting moments (Jolicoeur and Cardou, 1991). For the load range in which most of the steel wire cables are used (strains less than 0.01), the Velinsky (1985) concluded that the nonlinear theory showed no significant advantage over the linear theory (rod models).

Gysling (2008), using an incremental approach, validated the use of linear models to estimate axial cable capacity considering both linear and nonlinear material properties of the cable elements. Validation procedure was performed by using comparisons among different linear models reported by Jolicoeur and Cardou (1991), nonlinear model (Beltran, 2006) and experimental data on steel wire cables and polyester ropes. After extensive parameter studies on cables with different geometric parameters and with different constitutive materials behavior, the author concluded that linear models (fiber and rod models) are quite satisfactory to estimate overall cable response (cable stiffness, breaking axial load and breaking axial strain) for cables with helix angles less than 20º having both ends restricted to rotation.

From purely geometrical consideration, the linearized relationship of the wire axial strain e_i in terms of the cable axial strain e and the angle of twist per unit length f is given by

$$e_i = e\cos^2 q_{0i} + j a_{0i}\cos q_{0i}\sin q_{0i} \tag{2}$$

where a_{0i}; and $?_{0i}$ are the helix radius and the helix angle of wire i, respectively. As such, the linearized overall behavior of a cable subjected to axisymmetric loading can be written in the following incremental form:

$$\begin{pmatrix}\Delta F\\ \Delta M\end{pmatrix} = \begin{bmatrix}F_e & F_j\\ M_e & M_j\end{bmatrix}\cdot\begin{pmatrix}\Delta e\\ \Delta j\end{pmatrix} \tag{3}$$

where F_e, F_f, M_e, and M_f are the tangent stiffness coefficients; $?F$ and $?M$ are the increments in axial force and axial moment (torsion) respectively; and $?e$ and $?f$ are the increments in axial deformation and axial rotation per unit length respectively. Axial deformations are defined as follows: $?e = ?u/L$ and $?f = ??/L$ where $?u$ and $??$ are the axial displacement and axial rotation respectively (Fig. 6), and L is the initial cable length. For the sake of simplicity, considering the fiber model, tangent stiffness coefficients have the following form:

$$F_e = (AE)_c + \sum_{i=1}^{n}(AE)_i\cos^3 q_{0i} \tag{4a}$$

$$F_j = M_e = \sum_{i=1}^{n}(AE)_i a_{0i}\cos^2 q_{0i}\sin q_{0i} \tag{4b}$$

$$M_j = (GJ)_c + \sum_{i=1}^{n}(AE)_i a_{0i}^2\cos q_{0i}\sin^2 q_{0i} \tag{4c}$$

where subscript c refers to cable core; $(AE)_i$ is the axial stiffness of wire i, being A_i the cross-sectional area and E_i is the tangent modulus of wire i defined as $(ds/de)_i$ (tangent of the uniaxial stress-strain curve) for a given wire axial deformation e_i; and $(GJ)_c$ is the torsion stiffness of the core.

Based on the work by Motahari and Ghassemieh (2007), a multilinear one-dimensional pseudoelastic constitutive law is used for predicting the behavior of SMA wires under different loading conditions (Fig. 7). This model assumes a complete reverse transformation phase (path D-E in Fig. 7) and is described by six parameters: austenite elastic stiffness E_A; martensite elastic stiffness E_M; phase

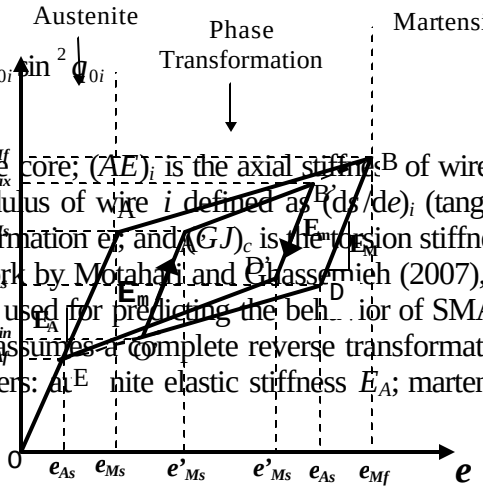

Fig. 7: Constitutive law of CuAlBe SMA wires

transformation starting stress s_{Ms}; phase transformation finishing stress s_{Mf}; and the unloading stress at the end of the reverse transformation s_{Af}. These parameters are obtained from experimental data on SMA wires.

The stress-strain relationships on different paths in Fig. 7 are as given as follows:

Paths O-A and E-O (elastic-fully austenite) $s = E_A e$ (5a)

Path A-B (forward transformation) $$s = s_{Ms} + \frac{s_{Mf} - s_{Ms}}{e_{Mf} - e_{Ms}}\left(e - e_{Ms}\right)$$ (5b)

Path B-D (fully martensite) $$s = s_{Mf} + E_M\left(e - e_{Mf}\right)$$ (5c)

Path D-E (reverse transformation) $$s = s_{As} + \frac{s_{Af} - s_{As}}{e_{Af} - e_{As}}\left(e - e_{As}\right)$$ (5d)

According to Motahari and Ghassemieh (2007), if the unloading occurs before the completion of the forward transformation or the reloading starts before completion of the reverse transformation, then the elastic stiffness is different from both austenite and martensite phases (paths O'-A', A'-B', B'-D' and D'-O'). The author proposed the following expression to estimate the tangent stiffness E_m (Fig. 7):

$$E_m = \frac{E_M E_A}{x\left(E_A - E_M\right) + E_M}$$ (6)

where x is defined as $(e_{max} - e_{Ms})/(e_{Mf} - e_{Ms})$ for the unloading case and $(e_{min} - e_{As})/(e_{As} - e_{Af})$ for the loading case. e_{max} and e_{min} are the maximum and minimum strains before unloading or reloading, respectively.

In Fig.8 comparisons between experimental data and predicted strand responses (based on the proposed analytical model) are presented for both types of strand construction: parallel and helical wire configuration for different strain ranges. The parameters used to define constitutive law of CuAlBe SMA wires are the following (Fig. 7): E_A = 57000 MPa; E_M = 32633 MPa; s_{Ms} = 340 MPa; s_{Mf} = 580.5 MPa; and s_{Af} = 180 MPa. Predicted responses estimate reasonable well the maximum strand axial stress for both types of strand constructions, especially for the case of parallel configuration. The analytical model, however, does not predict well the unloading path of the strand response, especially as the strain range increases. In fact, experimental data show the presence of residual strains which means that there is no complete reverse transformation. This phenomenon is not captured by the analytical model because a perfect pseudoleastic constitutive model is used to obtain predicted strand responses.

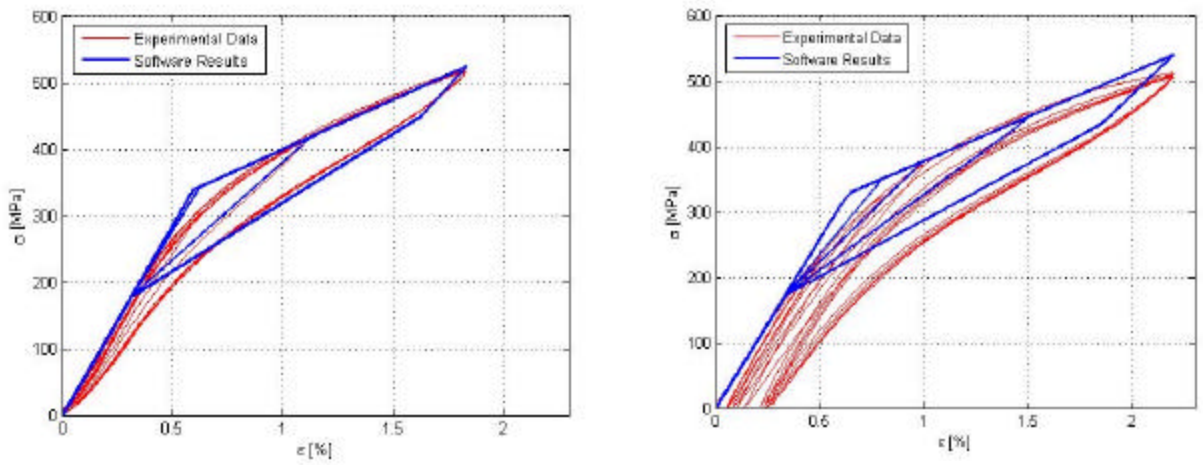

(a) Parallel wires (b) helical strand

Figure 8. Analytical and experimental results

Conclusions

This study evaluates the properties of cables and wires made of superelastic CuAlBe shape memory alloy under cyclic loading to assess its potential for applications in seismic resistant design. There are a number of additional challenges that must be overcome before going to an actual application including fabrication issues, such as the process of wounding and heat treating the cable, and cost issues. They have not been addressed in this work, considering that this is a first approach to assess the feasibility of using these cables.

Wires ϕ=0.5 mm, previously heated during different periods of time, are tested to study the effect of grain size, temperature and strain rate on the strength, equivalent viscous damping, and recentering properties of the alloy. The wires are subjected to quasi-static and dynamic tensile loading tests. The results show that nearly ideal superelastic properties can be obtained up to 3% axial strain. Overall, the damping potential of the alloy is moderate, typically less than 5%. Increased temperature lead to a reduction in the equivalent viscous damping and an increase in the forward transformation stress, while increased grain size lead to an increase in the equivalent viscous damping and a reduction in the forward transformation and ultimate stresses.

Strands made of helical and parallel wires were fabricated and tested in cyclic tension. Stress-strain curves resulted quite similar to those obtained for single wires. Equivalent viscous damping reaches up to 4%. Superelastic limit is about 3% showing good re-centering properties.

The maximum axial stresses are well predicted by the numerical model for both types of strand construction at every single strain cycle (values are overestimated less than 10% of the experimental values). The experimental data show, however, that strands do not have a complete reverse transformation phase which is not captured by the numerical model. Further research on the constitutive law model of CuAlBe SMA wires is needed to improve and validate the proposed numerical model.

Acknowledgments

This research has been funded by University of Chile and FONDECYT (grant nº 1070370 and 7070265). Special thanks to Dr. Reginald DesRoches for his kind permission to conduct the tests at Georgia Tech lab facilities.

References

Araya, R, M. Marivil, C. Mir, M. O. Moroni and A. Sepúlveda, 2008, Temperature and grain size effects on the behavior of CuAlBe SMA wires under cyclic loading, *Material Science and Engineering A* 6 (5), 725-801.

Beltran, J.F., 2006, Computational Modeling of Synthetic-Fiber Ropes, Ph.D. Dissertation, University of Texas at Austin, Austin, TX, USA.

Gysling, A., 2008, Numerical Comparison of Analytical Models to Predict Cable Behavior Under Axisymmetric Loads (in Spanish), University of Chile, Chile. ,

Jolicoeur, C., and Cardou, A., 1991, A Numerical Comparison of Current Mathematical Models of Twisted Wire Cables Under Axisymmetric Loads, *Journal of Energy Resources Technology*, 113, 241-249.

Motahari, S., and and Ghassemieh M., 2007, Multilinear One-dimensional Shape Memory Material Model for Use in Structural Engineering Applications, *Engineering Structures*, 29, 904-913.

Reedlunn B. and J. Shaw, 2008. Shape memory alloy cables. *Behavior and Mechanics of Multifunctional and Composite Materials, Vol. 6928.* SPIE.

Velinsky, S.A., 1985, General Nonlinear Theory for Complex Wire Rope, *International Journal of Mechanical Sciences*, 27, 497-507.